

Current Hysteresis Control of a Single Phase Integrated Battery Charger With Active Power Decoupling

Chunduri Sai Abhishek

Research advisor: Dr. R. Sudharshan Kaarthik



DEPARTMENT OF AVIONICS
INDIAN INSTITUTE OF SPACE SCIENCE AND TECHNOLOGY

November 18, 2021



Outline

- 1** Introduction
- 2** Integrated Battery Chargers
 - Single Phase FEC
 - Single Phase FEC Control Design
- 3** IBC Circuit Design
 - IBC Modes of Operation
 - Power Decoupling
 - Hysteresis Controller
 - Overall Control Architectures
- 4** Simulation Results
 - Steady State Results
 - Transient Response Results
 - Simulation Current Waveforms
- 5** Bibliography
 - References



Electric Vehicles and Classification

- Internal Combustion Engine vehicles burn fossil fuels like petrol and diesel to generate power.
- An electric vehicle (EV) is a vehicle that operates either partially or fully on electric power. Hence, they are considered to be eco-friendly.

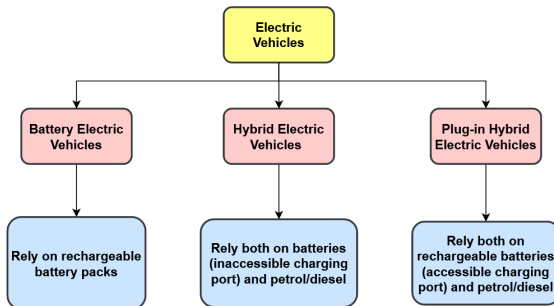


Figure 1: Classification of EVs.



Charging Infrastructures Available

S.No	Method of Charging	Category	Power	Time taken for Charging
1	On Board Chargers	Level - 1	1.4 kW	12 - 18 hours
2	Integrated Battery Chargers	Level - 2	3.3 - 6.6 kW	4 - 8 hours
3	Off Board Chargers	Level - 3	20 - 50 kW	15 - 30 minutes

Table 1: Classification of EV Charging Technologies. [1]

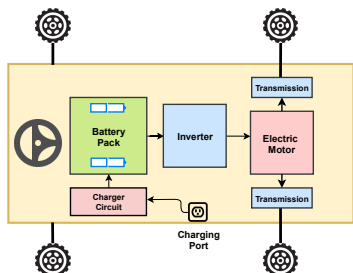


Figure 2: On-board Battery Charger.

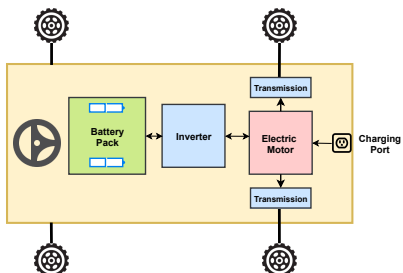


Figure 3: Integrated Battery Charger.



Power Train Configuration Used in EVs

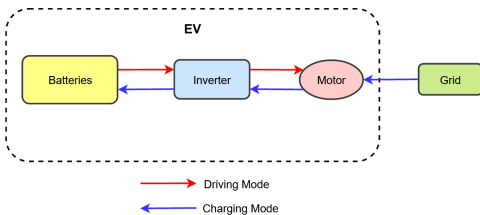


Figure 4: Power Flow in EV in driving and charging modes in an IBC.

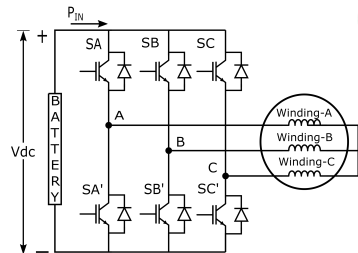


Figure 5: Typical Power Electronic Modules used in Electric Vehicles.



Need of Integrated Battery Chargers

- Vehicle will not be in both charging and driving mode at the same given instant.
- Use the traction hardware like motor and inverter, which are already present in the EV's powertrain, for charging the batteries.

Advantages of an IBC

- Reduced Cost
- Reduction in Weight
- Reduced Charging Time
- Charging from a single-phase power outlet
- Reduction in Footprint



Single Phase Front End Converter

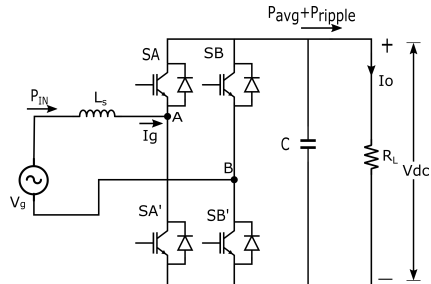


Figure 6: Single Phase Front End Converter Circuit.

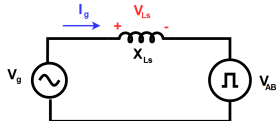


Figure 7: Single Phase FEC Equivalent Model.

- To Regulate the DC Bus Voltage (V_{DC})
- To Reduce the grid side current distortions
- To ensure bidirectional power flow and UPF operation [2]

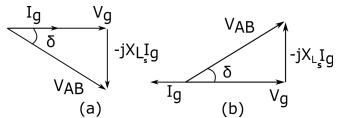


Figure 8: Phasor Diagram for : (a) UPF operation (AC-DC) (b) For reverse power flow at UPF (DC-AC).



Design Strategy

Equations related to Single Phase FEC

Input Power to the converter :

$$v_{AB}(t).i_g(t) = V_o i_{L_s}$$

$$v_{AB}(t).i_g(t) = V_{AB} \sin(\omega t).I_g \sin(\omega t - \theta)$$

$$i_{L_s} = \frac{V_{AB}.I_g}{2V_o} [\cos \theta - \cos(2\omega t - \theta)]$$

$$i_{L_s} = i_o + i_{cap}$$

$$i_{cap} = \frac{V_{AB}.I_g}{2V_o} \cos(2\omega t - \theta)$$

Design of Inductor (L_s)

Method – 1

$$|j\omega L_s I_g| \leq \frac{10}{100} V_g$$

Method – 2

$$V_g = j\omega L_s I_g + V_{AB}$$

$$V_{AB} = \sqrt{V_g^2 + (L_s \omega I_g)^2}$$

$$V_{AB} = m V_o$$

$$L_s \leq \sqrt{\frac{m^2 V_o^2 - V_{gmax}^2}{\omega^2 I_{gmax}^2}}$$

$m \rightarrow$ Modulation Index of SPWM

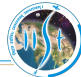
Design of DC Link Capacitor (C)

$$V_c(t) = \frac{i_c t}{C} = \frac{1}{C} \int_0^{\pi/2} I_g \cos(2\omega t) d(2\omega t) = \frac{I_g}{2C\omega}$$

$$\frac{I_g}{2C\omega} \leq \Delta V_o$$

$$C \geq \frac{m I_g}{8\pi f \Delta V_o}$$

$m \rightarrow$ Modulation Index of SPWM



Controller Design: Inner Current Loop

- PWM converter is modeled as a first-order transfer function with gain G .
- $T_c \rightarrow$ First Order Lag of the Controller
- $T_d \rightarrow$ Time period of one triangular carrier wave.

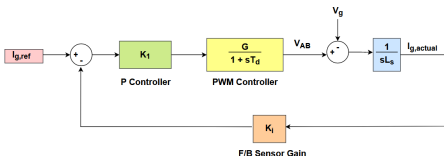


Figure 9: Inner Current Loop.

Inner Current Loop Transfer Function

$$G(s) = \frac{I_g}{I_{g\text{Ref}}} = \frac{K_1 G}{s^2 T_d L_s + sL_s + K_1 K_i G}$$

$$G(s) = \frac{\omega_n^2}{s^2 + 2\zeta\omega_n s + \omega_n^2}$$

$$2\zeta\omega_n = \frac{1}{T_d}, \omega_n^2 = \frac{K_1 K_i G}{T_d L_s}$$

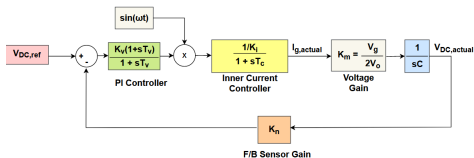
$$K_1 = \frac{L_s}{T_c K_i G}, \zeta = 0.707 \rightarrow T_c = 2 T_d$$

$$G_c(s) = \frac{\frac{1}{K_i}}{s^2 T_c T_d + s T_c + 1} \approx \frac{\frac{1}{K_i}}{s T_c + 1}$$



Controller Design: Outer Voltage Loop

- The objective of this controller is to ensure that the output DC bus voltage is at the desired value as per specifications.
- Assumption: The inner current loop acts much faster than the outer voltage loop. So, the inner current loop transfer function can be approximated to its first-order form.
- To design the voltage controller, third-order modulus hugging method is used.



Outer Voltage Loop Transfer Function

$$H(s) = \frac{V_{DC}}{V_{DC,Ref}}$$

$$H(s) = \frac{sV_g T_v K_v + V_g K_v}{V_g K_n K_v + s(K_n K_v V_g T_v) + s^2(2K_i T_v V_o C) + s^3(2K_i T_v T_c V_o C)}$$

$$K_v = \frac{4K_i V_o C}{K_n V_g T_v}$$

$$T_v = 4T_c = 4(2T_d) = 8T_d$$

Figure 10: Outer Voltage Loop.



IBC Circuit and Modes of Operation

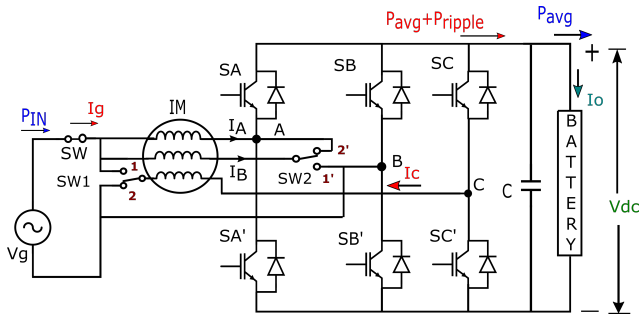


Figure 11: Integrated Battery Charger Circuit.

S.No	Mode of Operation of EV	SW Position	SW ₁ Position	SW ₂ Position
1	Driving Mode (Motoring Mode)	Open	1	1'
2	Charging Mode	Close	2	2'

Table 2: Switch Positions in different modes of operation.



Figure 12: Relay Switches used for SW , SW_1 , and SW_2 .



IBC Configuration in Different Modes

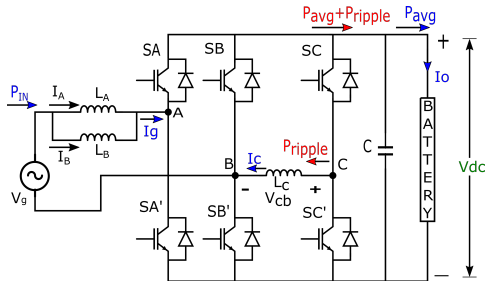


Figure 13: IBC Circuit in Charging Mode.

Driving Mode

- Legs A, B, and C act as a load to the 3- ϕ inverter, which is powered by the EV's battery.

Charging Mode

- Windings A and B of IM are connected in parallel and serve as interface inductors for the 1- ϕ grid.
- The C-phase winding acts as a decoupling inductor for the active power decoupling circuit to minimize DC bus voltage ripple.



Why is Power Decoupling Needed ?

Power Decoupling Equations

$$V_{in}(t) = V_g \cos \omega t$$

$$I_{in}(t) = I_g \cos \omega t$$

$$P_{in}(t) = V_{in}(t).I_{in}(t) = \frac{V_g \cdot I_g}{2} + \frac{V_g \cdot I_g \cdot \cos(2\omega t)}{2}$$

$$P_{in} = P_{avg} + P_{ripple} = P_{out}$$

- P_{avg} is the power consumed by the load, and P_{ripple} appears across the DC bus.
- This causes a ripple of twice frequency to that of fundamental in DC bus voltage.
- This ripple affects the performance of the DC bus capacitor (causes heating of capacitor), leading to its shorter lifetime.



Power Decoupling Analysis

Mathematical Equations

Assuming that reference decoupling current through L_C as :

$$i_{LC} = I_{LC} \sin(\omega t + \alpha) \quad \text{and} \quad P_{LC} = L_C \left(\frac{di_{LC}}{dt} \right) i_{LC} = \omega L_C I_{LC}^2 \sin(2\omega t + 2\alpha)$$

From power balance principle,

$$P_{inst} = P_{Load} + 2P_{LA} + P_{LC}$$

$$P_{Load} + \frac{\omega L_A I_m^2 \sin(2\omega t)}{4} + \frac{\omega L_C I_{LC}^2 \sin(2\omega t + 2\alpha)}{2} = \frac{V_m \cdot I_m}{2} + \frac{V_m \cdot I_m \cdot \cos(2\omega t)}{2}$$

Defining, $\phi = \tan^{-1} \left(\frac{\omega L_A I_m}{2V_m} \right)$

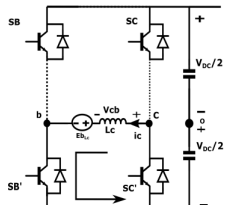
We get, $I_{LC} = \sqrt{\frac{(V_m I_m)^2 + \left(\frac{\omega L_C I_m^2}{2} \right)^2}{\omega L_C}}$ and $\alpha = \frac{-\phi}{2} - \frac{\pi}{4}$

For input current at UPF operation,

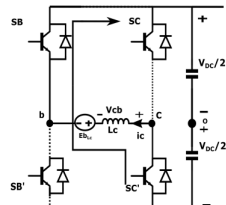
$$\alpha \approx \frac{\pi}{4}$$



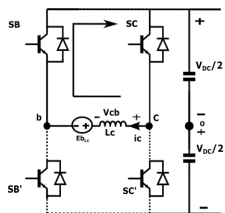
Active Power Decoupling Scheme



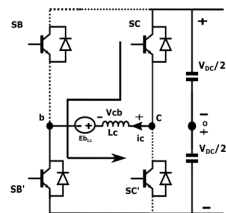
(a) Mode I



(b) Mode II



(c) Mode III



(d) Mode IV

Figure 14: Different modes of the operation of power decoupling.



Operation of Power Decoupling

S.No	Mode	SB	SB'	SC	SC'	v_{L_c}
1	Mode I	OFF	ON	OFF	ON	Zero
2	Mode II (Discharging Mode)	ON	OFF	OFF	ON	$-V_{DC}$
3	Mode III	ON	OFF	ON	OFF	Zero
4	Mode IV (Charging Mode)	OFF	ON	ON	OFF	V_{DC}

Table 3: Switch Positions for different modes of the operation of power decoupling.

- Power decoupling works in a way that, when $P_{in}(t) > P_{avg}$, P_{ripple} flows through DC bus capacitor and when $P_{in}(t) \leq P_{avg}$, P_{ripple} flows back to grid from DC bus capacitor.



Hysteresis Controller

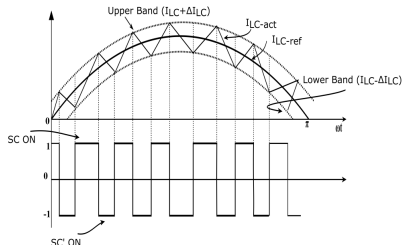


Figure 15: Switching Pulse Generation for C Winding via Hysteresis Controller.

Working Logic

- For the simulation case, an error of 500mA from nominal decoupling current is considered.
- Whenever I_{dec} hits the upper band, the hysteresis controller generates a low switching pulse for the top IGBT device and a high pulse for the bottom IGBT device of the C phase the opposite happens when I_{dec} hits the lower band.
- This switching sequence causes diversion of ripple power in the decoupling inductor, and hence ripple in DC bus voltage is minimized.

Advantages

- Excellent dynamic performance and ability to control the peak to peak value of current ripple in desired hysteresis band.
- Inherent short circuit protection for grid current.
- Easier controller implementation.



Conventional Overall Control Scheme

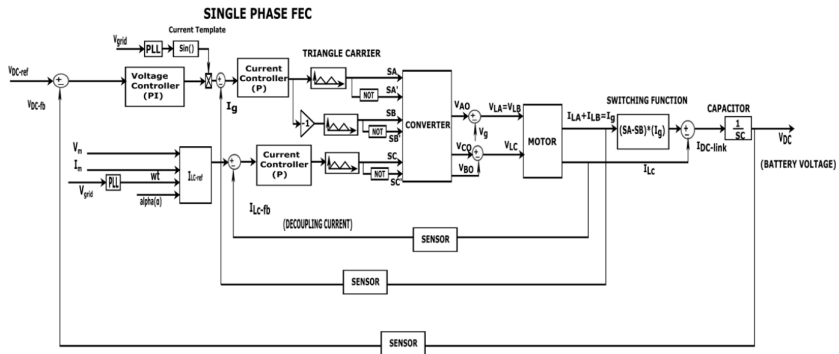


Figure 16: Conventional Control scheme for IBC topology with decoupling.



Hysteresis Based Overall Control Scheme

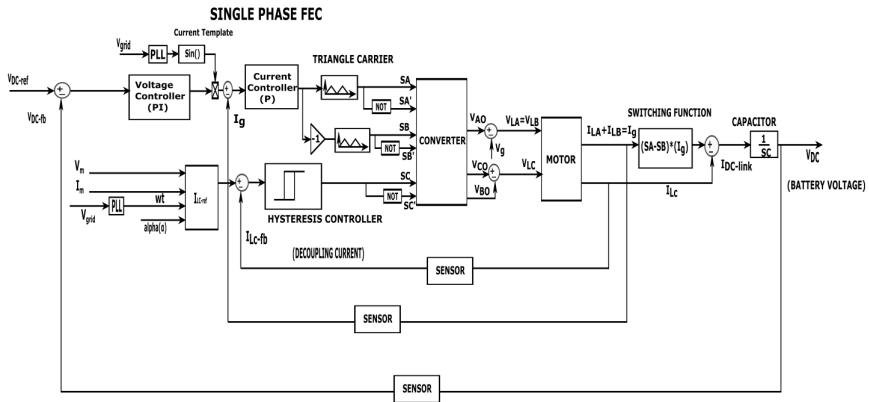


Figure 17: Control scheme for IBC topology using Hysteresis controller.

Simulation Results



Parameters	Variable	Value
Grid Voltage	V_g	230V(rms)
DC link Voltage	V_{DC}	400V
DC link Capacitance	C	800uF
Switching frequency	f_s	10KHz
Max.Power	P_{out}	2kW
Motor stator leakage inductance	L_s	10mH
Motor rotor leakage inductance	L_r	10mH
Motor mutual inductance	L_m	82mH
Stator resistance	R_s	1Ω
Rotor resistance	R_r	1.1Ω

Table 4 : Simulation Parameters for IBC Simulation.



Steady State Response of IBC

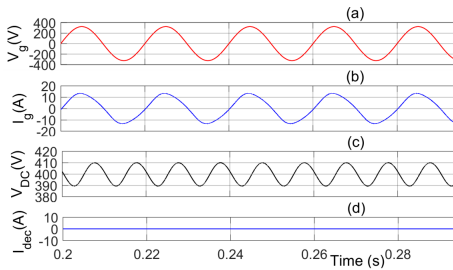


Figure 18: Steady state waveforms for 1- ϕ FEC without decoupling.

→ Voltage Ripple = $\pm 10V$

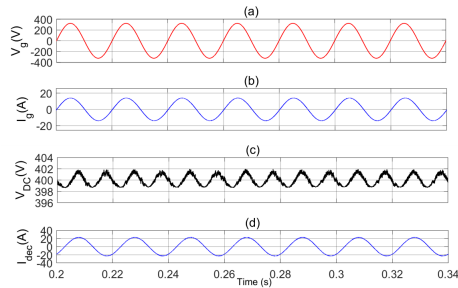


Figure 19: Steady state waveforms for 1- ϕ FEC with decoupling.

→ Voltage Ripple = $\pm 2V$



Transient Behaviour of IBC

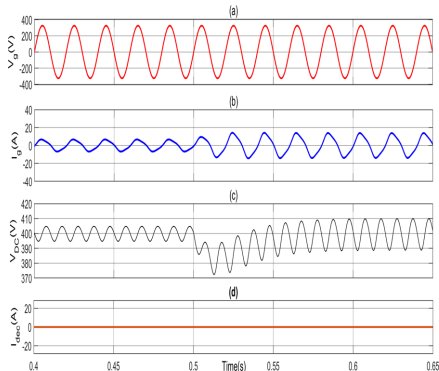


Figure 20: Transient waveforms for step load change from half load to full load at time $t = 0.5$ s without decoupling (**Step-Response**).

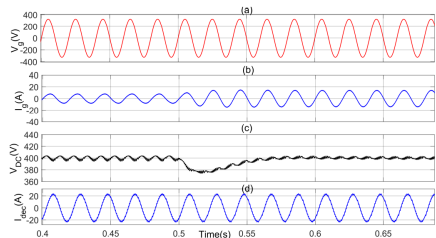


Figure 21: Transient waveforms for step load change from half load to full load at time $t = 0.5$ s with decoupling (**Step-Response**).



Transient Behaviour of IBC

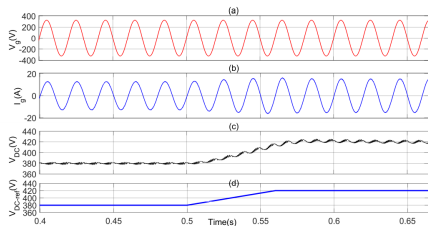


Figure 22: Transient waveforms for a uniform increase in reference DC bus voltage (from 380 V to 420 V) for three cycles with decoupling (**Ramp-Up Response**).

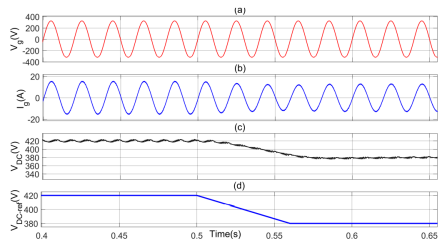


Figure 23: Transient waveforms for a uniform increase in reference DC bus voltage (from 380 V to 420 V) for three cycles with decoupling (**Ramp-Down Response**).



Simulation Current Waveforms

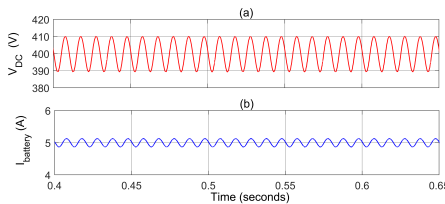


Figure 24: Steady state waveforms without decoupling. (a) DC-bus Voltage (V_{DC}) (b) Battery Current ($I_{battery}$).

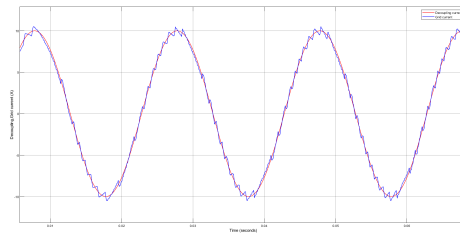


Figure 25: Current Hysteresis Control in action. I_{dec} tracks the grid current within the hysteresis margin



Simulation Current Waveforms

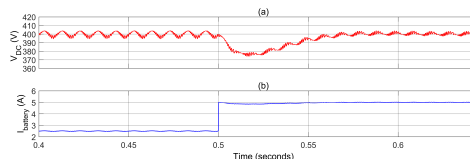


Figure 26: Transient waveforms for step change in load from half load to rated load at $t = 0.5$ sec with decoupling. (a) DC-bus Voltage (V_{DC}) (b) Battery Current ($I_{battery}$).

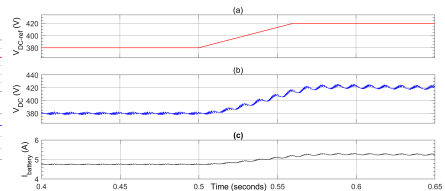


Figure 27: Transient waveforms for change in reference DC-bus voltage with decoupling . (a) DC-bus ref Voltage (V_{DC_ref}) (b) DC-bus Voltage (V_{DC}) (c)Battery Current ($I_{battery}$).

Paper Accepted for IEEE PESGRE 2022 Conference

- Title: Current Hysteresis Control of a Single Phase Integrated Battery Charger With Active Power Decoupling
- Authors: Mohit Kumar, Chunduri Sai Abhishek, R. Sudharshan Kaarthik, *Senior Member, IEEE*

References



- [1] Mallikarjun Kompella, Pragya Yadav, and R. Sudharshan Kaarthik. "A Single Phase Integrated Battery Charger with Active Power Decoupling for Electric Vehicles". In: *2020 IEEE International Conference on Power Electronics, Drives and Energy Systems (PEDES)*. 2020, pp. 1–6. DOI: [10.1109/PEDES49360.2020.9379459](https://doi.org/10.1109/PEDES49360.2020.9379459).
- [2] Saumya Tripathi and Rupanshi Batra. "Operation and Control of Single Phase Front End Converter". In: *2020 First IEEE International Conference on Measurement, Instrumentation, Control and Automation (ICMICA)*. 2020, pp. 1–6. DOI: [10.1109/ICMICA48462.2020.9242832](https://doi.org/10.1109/ICMICA48462.2020.9242832).



Thank You

Questions ?